

Energy and Angular Distribution of Alpha-Particles in the $\text{Ar}^{40}(n, \alpha)\text{S}^{37}$ Reaction at 14.1 Mev.*

YUIN-CHI HSÜ (許雲基), CHIA-YI HUANG (黃家裕)

CHAO-YANG HUANG (黃昭陽) and SONG-YUNG LIN (林松雲)

Department of Physics, National Taiwan University, Taipei, Taiwan

(Received October 30, 1965 j)

The energy and angular distribution of alpha-particles from the $\text{Ar}^{40}(n, \alpha)\text{S}^{37}$ reaction induced by 14.1 Mev neutrons were measured with an argon-gas filled cloud chamber. The angular distribution for the entire energy region is approximately symmetrical with 90° and concave upward. The energy distribution shows that the alpha-particles are more emitted than has been expected from the statistical theory.

Values for the level density parameter a , the nuclear temperature T and the spin cut-off parameter σ are evaluated from these data.

I. INTRODUCTION

MUCH more information exists about the total cross section of the (n, α) reactions at 14 Mev⁽¹⁻³⁾. These cross sections have been measured mainly by means of the activation method. An analysis of these data shows that for medium weight nuclei, the (n, α) reactions at 14 Mev seem to proceed mainly through the compound nucleus⁽⁴⁾. Total cross section measurements by themselves are, however, insufficient to give reliable information on the mechanism of the (n, α) reaction. The research has been extended to the energy and angular distribution to get detailed information of the (n, α) reaction mechanism, but the existing experimental data are still rather scarce.

The main reasons for this situation are the experimental difficulties which arise from the background problems, from the particle discrimination and from the smallness of the cross section. In most cases the alpha-particles have been detected by means of: (a) nuclear emulsion method⁽⁵⁻¹⁴⁾ in which proper methods

* Supported partly by the National Council on Science Development.

(1) Peter R Gray, Arlen R. Zander and Thomas G. Ebrey, Nuclear Physics 62, 172 (1965).

(2) A. Chatterjee, Nucleonics 22, No. 8, 108 (1964).

(3) Donald G. Gardner and Yu-wen Yu, Nuclear Physics 60, 49 (1964).

(4) U. Facchini, E. Saetta-Menichella, F. Tonoli and F. Tonolini-Serergnini, Nuclear Physics 51, 460 (1964).

(5) A. H. Armstrong and J. E. Brolley, Jr., Phys. Rev. 99, 330 (1955).

(6) I. Kumabe, E. Takekoshi, H. Ogata, Y. Tsuneoka, and S. dki, Phys. Rev. 106, 155 (1957) and J. Phys. Soc. Japan 13, 129 (1958).

(7) Isao Kumabe, J. Phys. Soc. Japan 13, 325 (1958).

(8) B. Sen, Nuclear Physics 38, 601 (1962); 41, 439 (1963).

(9) O. N. Kaul, Nuclear Physics 39, 325 (1962); 55, 263 (1964).

for developing the plates have been employed in order to discriminate the alpha-particles from other charged particles, (b) counter telescope^(15,16) consisting of proportional and scintillation counter or thin and thick detectors as dE/dx and E counters, and (c) the pulse-shape discrimination method^(17,18) to distinguish the alpha-particles.

In some cases in which gases, especially, inert gases are to be studied, it seems that cloud chamber-is most suitable; one of the first and best studies was made by Lillie⁽¹⁹⁾, who investigated the $\text{O}^{16}(n,\alpha)\text{C}^{13}$ and $\text{N}^{14}(n,\alpha)\text{B}^{11}$ reactions. Recently Gray et al.⁽¹⁾ have reported the total cross section for the $\text{Ar}^{40}(n,\alpha)\text{S}^{37}$ reaction, but the energy and angular distribution of alpha-particles from this reaction have not been known to the authors. In the present work carried out with a cloud chamber, we investigated the $\text{Ar}^{40}(n,\alpha)\text{S}^{37}$ reaction and evaluated some statistical parameters from the energy and angular distribution data observed.

II. EXPERIMENTAL PROCEDURE

The 14.1 Mev neutrons were produced by a 200 kv Cockcroft-Walton accelerator using the $\text{T}(d,n)\text{He}^4$ reaction. The experimental arrangement is shown in Fig. 1. The neutrons entered the cloud chamber at 90° to the deuteron beam. The chamber of rubber diaphragm type was 40 cm in diameter by 20 cm deep. The center of the chamber was placed 50cm from the center of the Zr-T target and 90 cm from the floor. Argon-gas having less than one percent impurities filled the cloud chamber to a pressure of one atmosphere and water vapor was used as the vapor in the chamber. An electric field of approximately 50 volts/cm was applied across the chamber for clearing.

Stereoscopic pictures of the tracks in the chamber were taken using two cameras. The illumination was obtained by discharging a condenser bank of 133 μf at 2,000 volts through a pair of flash tubes which were connected in series. The flash tube having an inner diameter of 0.7 cm and length of 25 cm was filled with xenon-gas up to a pressure of 4 cmHg and was placed at the focus of a parabolic reflector to provide a parallel beam. Since the cameras were used with opened shutter, the length of the exposure was determined simply

(10) W. Patzak and H. Vonach, Nuclear Physics 39, 263 (1962).

(11) C. J. D. Jarvis, W. R. Dixon and R. S. Storey, Nuclear Physics 44, 680 (1963).

(12) R. A. Al-Kital and R. A. Peck, Jr., Phys. Rev. 130, 1500 (1963).

(13) M. L. Chatterjee and B. Sen, Nuclear Physics 51, 583 (1964).

(14) K. Breuer and E. Rössle, Nuclear Physics 69, 587 (1965).

(15) F. L. Ribe and W. Davis, Phys. Rev. 99, 331 (1955).

(16) P. Kulišić, V. Ajdačić, N. Cindro, B. Lalović and P. Strohal, Nuclear Physics 54, 17 (1964).

(17) W. R. Dixon, Nuclear Physics 42, 27 (1963).

(18) U. Seebeck and M. Borman, Nuclear Physics 68, 387 (1965).

(19) Allan B. Lillie, Phys. Rev. 87, 716 (1952).

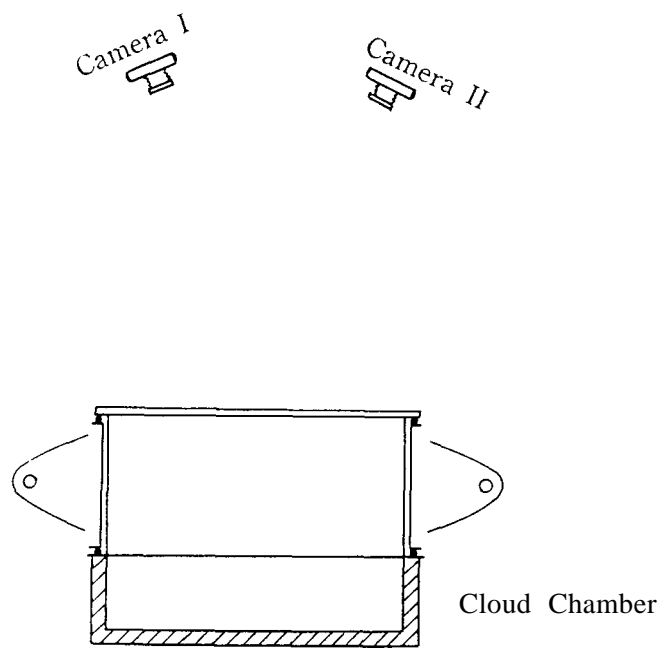


Fig. 1. Cloud chamber with the camera system.

by length of the flash, which was estimated to be of the order of 10^{-4} sec. The film used was Kodak Plus-X Pan, and processed with F-19 developer in order to increase photographic contrast. Fig. 2 shows an example of such stereoscopic picture.

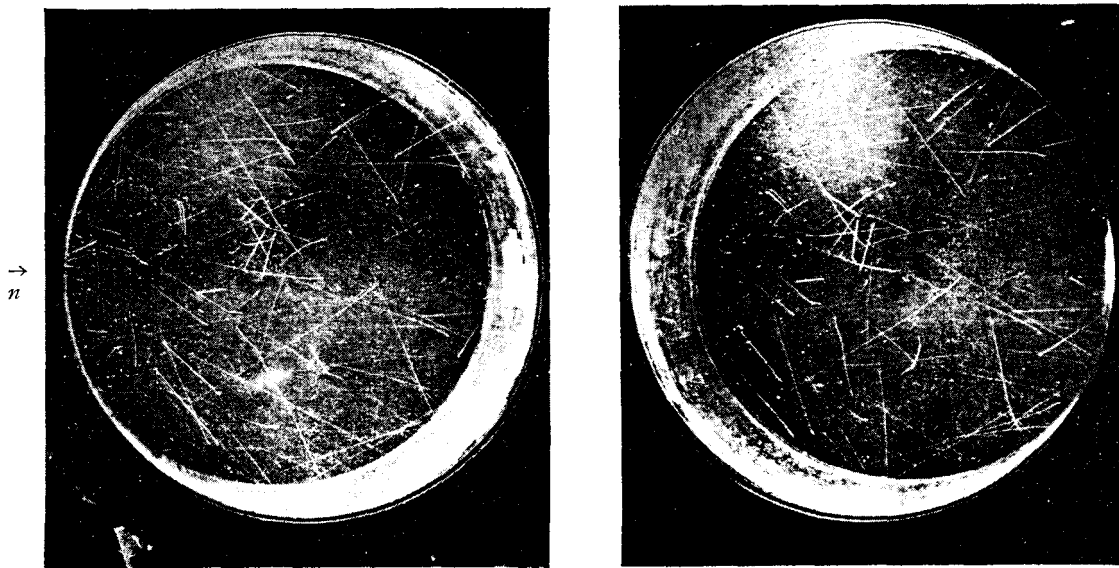


Fig. 2. An example of the stereoscopic picture of disintegrations produced by 11.1 Mev neutrons. The arrow indicates their direction of incidence. The chamber is filled with 1 atmos. argon-gas and water mixture. ($f=16$, Kodak Plus-X Pan).

Measurements of track lengths and the angles that the tracks made with the neutron's paths were performed by reprojecting the films through the same optical system as these were taken. The position of the screen on which the two projected images appear is adjusted until they coincide, then the length and position of the image are the same as those occurred actually.

Since the momentum, before and after the nuclear reaction, should be conserved, a fork consisting of the alpha-particle and the residual S^{37} must lie on a plane passing through the Zr-T target. If the disintegration were caused by scattered neutron or if two particle emitting reaction had taken, the plane of the fork would not pass through the target position. In addition, the track of alpha-particle can easily be distinguished from other charged particles by the relative track densities. All forks were recorded provided the plane of the fork was less than 60° to the horizontal and the origin of the fork was located in a cylinder of radius 15 cm measured from the center of the chamber. The measured length of the alpha-particle track was, then, converted into energy using the range-energy table of Ward Whaling⁽²⁰⁾.

III. RESULTS AND DISCUSSION

Since, in the present work, water vapor was used as the chamber vapor, the overall alpha-particle tracks obtained from the bombardment of argon-gas containing appreciable amount of oxygen atoms would be due to the combined contributions from the $\text{Ar}^{40}(n, \alpha)\text{S}^{37}$ and $\text{O}^{16}(n, \alpha)\text{C}^{13}$ reactions. So to obtain exclusively the contribution of the $\text{Ar}^{40}(n, \alpha)\text{S}^{37}$ reaction, the effects of the $\text{O}^{16}(n, \alpha)\text{C}^{13}$ reaction should be eliminated using the data already published; for this purpose the work of Lillie⁽¹⁹⁾ was applied.

Fig. 3 shows the energy distribution of alpha-particles against the energies in the center of mass system as well as the excitation energies of residual S^{37} . Positions of levels in the literature⁽²¹⁾ are also indicated. The angular distribution of the alpha-particles from the $\text{Ar}^{40}(n, \alpha)\text{S}^{37}$ reaction in the center of mass system for the entire energy region is shown in Fig. 4. The distribution is approximately symmetric with respect to 90° . The solid curve represents the least-square fit of the observed angular distribution by an expression of the form $A + B \cos^2 \theta$.

The energy and angular distribution have been analyzed on the basis of statistical model. The energy distribution of the alpha-particles emitted in the compound nuclear reaction can be written by Weisskopf formula⁽²²⁾,

(20) S. Flügge, *Encyclopedia of Physics*, XXXIV, Corpuscles and Radiation in Matter II (Springer-Verlag, 1958) p. 193.

(21) P.M. Endt and C. M. Brans, *Revs. Modern Phys.* **29**, 683 (1957).

(22) J. M. Blatt and V. F. Weisskopf, *Theoretical Nuclear Physics* (John Wiley and Sons, Inc., New York, 1952) p. 353.

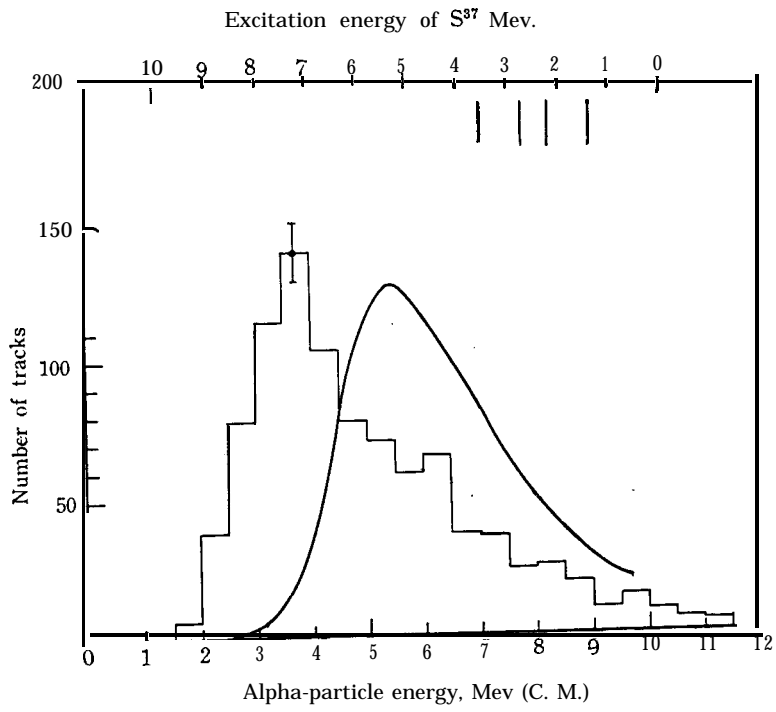


Fig. 3. Energy distribution of alpha-particles from the $\text{Ar}^{40}(n, \alpha)\text{S}^{37}$ reaction. The contribution from the $\text{O}^{16}(n, \alpha)\text{C}^{13}$ reaction has been subtracted.

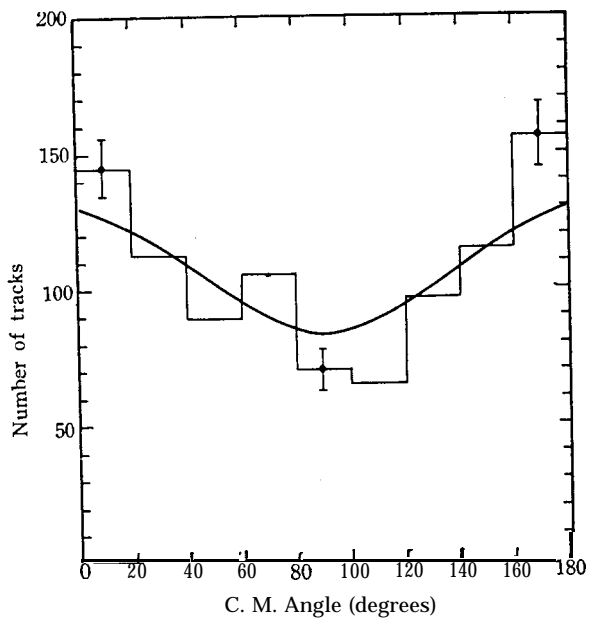


Fig. 4. Angular distribution of alpha-particles from the $\text{Ar}^{40}(n, \alpha)$ reaction.

$$N(\epsilon_\alpha)d\epsilon_\alpha = \text{const} \cdot \epsilon_\alpha \sigma_c(\epsilon_\alpha) \omega(E) d\epsilon_\alpha, \quad (1)$$

where $N(\epsilon_\alpha)d\epsilon_\alpha$ is the number of alpha-particles emitted with energies between ϵ_α and $\epsilon_\alpha + d\epsilon_\alpha$, $\sigma_c(\epsilon_\alpha)$ is the cross section for the formation of the compound

nucleus in the same state of excitation by the reverse reaction in which alpha-particles of energy ε_α strike the excited residual nucleus, and $\rho(E)$ is the level density of the residual nucleus at the excitation energy E . For the level density $\omega(E)^{(23)}$, we put

$$\omega(E) \propto E^{-2} \exp(2\sqrt{aE}), \quad (2)$$

with a as an energy independent level density parameter.

In order to analyze the observed spectra, the natural logarithm of the so-called reduced spectrum $\frac{NE^2}{\varepsilon_\alpha \sigma_c(\varepsilon_\alpha)}$ is introduced to result in

$$\ln \left[\frac{N(\varepsilon_\alpha)E^2}{\varepsilon_\alpha \sigma_c(\varepsilon_\alpha)} \right] \propto 2\sqrt{a} \cdot \sqrt{E}. \quad (3)$$

In Fig. 5 are given the statistical plots $\log_{10} \frac{NE^2}{\varepsilon_\alpha \sigma_c}$ as a function of $E^{1/2}$ for the entire energy region of alpha-particles. The resulting curve would be a straight line and the slope of the line has a value of $2\sqrt{a} \log_{10} e$.

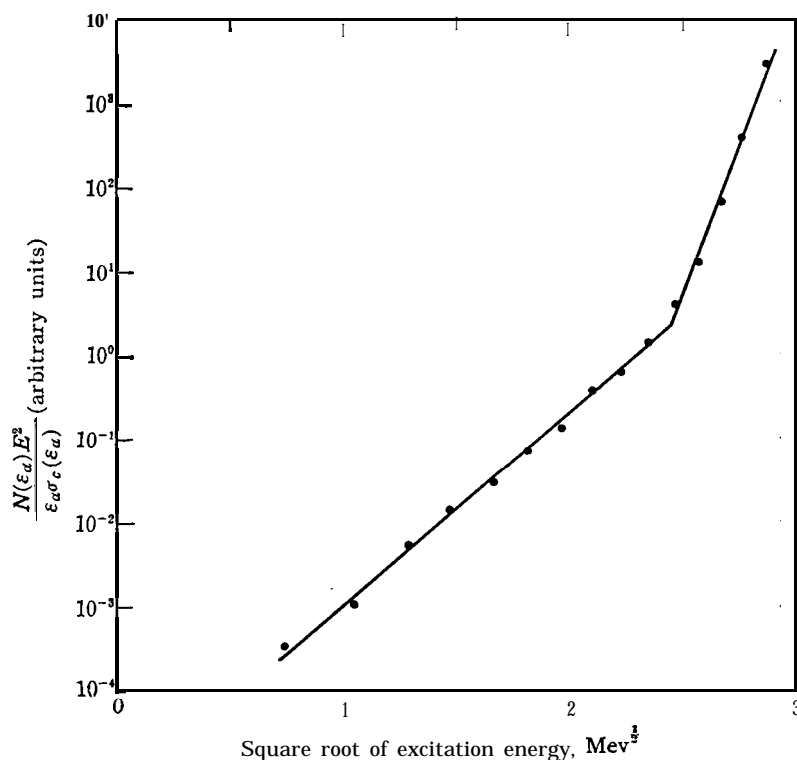


Fig. 5. Statistical plots of alpha-particle spectra.

For the inverse cross section $\sigma_c(\varepsilon_\alpha)$, we have employed the optical model cross

(23) T. Ericson, Phil. Mag. Suppl. 9, 425 (1960).

sections obtained by Huizenga and Igo⁽²⁴⁾. From the slope of the straight line a value of $a=6.4 \pm 0.3 \text{ Mev}^{-1}$ is deduced for the level density parameter. The solid curve in Fig. 3 represents

$$N(\varepsilon_\alpha) = \text{const} \cdot \varepsilon_\alpha \sigma_c(\varepsilon_\alpha) E^{-2} \exp(2\sqrt{aE})$$

with the calculated value of a , where the area enclosed by the curve is normalized to the total number of alpha-particles observed.

In Fig. 5 the experimental points define a straight line on average. But at higher excitation energies there appears a systematic deviation from this line. From the consideration of Q -values and Coulomb barrier effect, three reactions are expected to contribute to the alpha-particle emission observed from the ($\text{Ar}^{40} + n$) reaction: $\text{Ar}^{40}(n, \alpha)\text{S}^{37}$, $\text{Ar}^{40}(n, \alpha n')\text{S}^{36}$ and $\text{Ar}^{40}(n, n'\alpha)\text{S}^{36}$ ($Q(n, n'\alpha) = -2.42 \text{ Mev}^{(25)}$, $Q(n, \alpha n') = Q(n, n'\alpha) = -7.15 \text{ Mev}$).

The contributions from the first two reactions cannot be distinguished in the statistical plots. Many investigators have found the same deviation and attributed this situation to the ($n, n'\alpha$) reaction, since it is impossible to determine through which reaction the alpha-particles are emitted. In the present work, the plane of the fork for the ($n, n'\alpha$) reaction cannot pass through the Zr-T target position, so, in principle, it is expected that the ($n, n'\alpha$) reaction can be eliminated. However, it should be remarked there are some possibilities that the alpha-particles from the ($n, n'\alpha$) reaction may mix up with those from the (n, α) reaction, since it is sometimes difficult to determine whether the plane of the fork does pass through the Zr-T target because of the short range of the residual nucleus. The cross sections $\sigma_c(\varepsilon_\alpha)$ used are those obtained by Huizenga and Igo⁽²⁴⁾ with the appropriate optical model potential. It should be pointed out, however, that the inverse cross sections for alpha-particle are particularly sensitive to the parameters of the optical model for energies below the classical barriers. In addition, we have evaluated the values for σ_c by interpolating the values given by Huizenga et al. From the above stated, therefore, the deviation from the straight line in the statistical plot may be ascribed to the ($n, n'\alpha$) reaction and the ambiguities of σ_c which has important effect on the plot.

The angular distribution has been compared with the formula derived as the first order approximation by Ericson^(23, 26)

$$W(\theta) = 1 + \frac{1}{12} \cdot \frac{\bar{J}^2 \cdot \bar{l}^2}{\sigma^4} P_2(\cos \theta). \quad (4)$$

$W(\theta)$ is the relative angular distribution, $P_2(\cos \theta)$ is the second Legendre polynomial and σ denotes the spin cut-off parameter for the residual nucleus. J

(24) J. R. Huizenga and G. Igo, Nuclear Physics 29, 462 (1962); Report ANL-6373.

(25) F. Everling, L. A. Koenig, J. H. E. Mattauch and A. H. Wapstra, *Nuclear Data Tables* (United States Atomic Energy Commission, 1960).

(26) T. Ericson and V. Strutinski, Nuclear Physics 8, 284 (1958).

is the spin of the compound nucleus and l is the orbital angular momentum of the emitted particle. The bars indicate averages taken with weight factors $(2J+1)T_l(\epsilon_n)$ and $(2l+1)T_l(\epsilon_\alpha)$ for J^2 and l^2 , where the quantities $T_l(\epsilon_n)$ and $T_l(\epsilon_\alpha)$ are the transmission coefficients for the incident neutrons and the emitted alpha-particles, respectively. For $T_l(\epsilon_n)$ values, the results of W. S. Emmerich⁽²⁷⁾ were taken, and for $T_l(\epsilon_\alpha)$ the work of Huizenga et al.⁽²⁴⁾ were used. A value of 123 was obtained for the product $\bar{J}^2 \cdot \bar{l}^2$.

For the purposes of evaluating the spin cut-off parameter σ the entire energy region was applied assuming that the alpha-particles are emitted through the (n, α) reaction. The observed angular distribution has been fitted by the least-square method to the form $A+B\cos^2\theta$ with the values

$$A=84.7 \pm 10.0 \text{ and } B=42.8 \pm 15.5.$$

These values have led to a spin cut-off parameter of $\sigma=2.4_{-0.2}^{+0.4}$ for the residual nucleus.

The spin cut-off parameter is related with the nuclear temperature T by

$$\sigma^2 = \frac{TI}{\hbar^2}, \quad (5)$$

where I denotes the moment of inertia of the nucleus and T is given by

$$\frac{1}{T} = \frac{d}{dE}[\ln\omega(E)] = -\frac{2}{E} + \sqrt{\frac{a}{E}}. \quad (6)$$

Using the excitation energy of the product nucleus which belongs to the maximum of the evaporation spectrum, and the level density parameter a obtained from the statistical plot, a value of $T=1.50 \pm 0.05$ is evaluated for nuclear temperature of residual nucleus. Applying an independent particle model with a square well potential of radius R , Bloch⁽²⁸⁾ derived the relation

$$I_R = \frac{2}{5}MAR^2, \quad (7)$$

where A is the mass number and M the mass of a nucleon. This corresponds to the moment of inertia of a rigid sphere which is expected to reach for higher excitation energies. Using σ and T , the moment of inertia I can be evaluated by eq. (5) and is compared with I_R in eq. (7). For the radius $r_0=1.2$ fm, the ratio I/I_R becomes 0.7 and for $r_0=1.5$ fm the ratio is 0.4, respectively.

IV. ACKNOWLEDGMENT

The authors are deeply indebted to Prof. Jenn-Lin Hwang for his valuable discussion.

(27) J. B. Marion and J. L. Follower, *Fast Neutron Physics*, Part II (Interscience Publishers, 1963) p. 1057.

(28) C. Bloch, *Phys. Rev.* 93, 1094 (1954).